Remote Sensing of Environment 136 (2013) 126–134

Contents lists available at SciVerse ScienceDirect

Remote Sensing of Environment

journal homepage: www.elsevier.com/locate/rse

Landsat-based early warning system to detect the destruction of villages in Darfur, Sudan

A.J. Marx *,[1], T.V. Loboda

Department of Geographical Sciences, University of Maryland, 2181 Samuel J. LeFrak Hall College Park, MD, 20742, USA

ARTICLE INFO

Article history:
Received 6 February 2013
Received in revised form 30 April 2013
Accepted 1 May 2013
Available online 28 May 2013

Keywords:
Landsat
Human rights
Darfur, Sudan
Arid environments

ABSTRACT

Organizations concerned with human rights are increasingly using remote sensing as a tool to improve their detection of human rights violations. However, as these organizations have transitioned to human-rights monitoring campaigns conducted over large regions and extended periods of time, current methods of using high-resolution sensors and manpower-intensive analyses have become prohibitive. We present an algorithmic approach that uses Landsat ETM+, coupled with high-resolution sensors, as a system for the detection of the destruction of villages in arid environments. This algorithm capitalizes on Landsat's historical archive and systematic observations by constructing a historic spectral baseline for each village in the study area. This allows for the automated detection of a potentially destroyed village with each new overpass of the sensor. The algorithm is based on Landsat's near-infrared band, which is a persistent indicator of the destruction of plant cell structure, and is less affected by atmospheric scattering than Landsat's visible bands. Comparison of this product with a U.S. government database documenting destroyed villages shows high levels of accuracy among villages in the study area. We evaluated algorithm performance in Darfur, Sudan for the 2004 calendar year. In the study area, the Landsat estimates were within 16% of the U.S. government database, demonstrating a functioning system to alert human rights practitioners to a potential destruction of villages.

Published by Elsevier Inc.

1. Introduction

In response to the crimes committed against humanity during the Second World War, the global community, through the newly formed United Nations (U.N.), drafted the Universal Declaration of Human Rights to identify and establish a mandate to protect universal human rights. Today the U.N., along with other governmental and non-governmental organizations (NGOs), conducts imagery-based human rights monitoring campaigns to document any governmental and non-state transgressions and abuses of human rights and the failures of the state to protect these rights (Marx & Goward, 2013; Office of the High Commissioner for Human Rights, 2001). These campaigns are systematic, long-term efforts over a large region, using tens or hundreds of satellites images to detect phenomena associated with violations of human rights and international humanitarian law. Satellite observations have remedied biases in human ecology studies related to difficulty of accessing many remote areas and subsequent preferential sampling of sites in proximity to roads and reliance on single snapshot observations in characterizing those sites; however, they have only partially removed another major limitation of human ecology research — heavy reliance on visual description of patterns (Turner, 2003).

Although very high resolution (VHR) (10 meter and higher spatial resolution) imagery has been used in since the 1990s to document specific human rights events such as the 1995 massacre in Srebrenica, Bosnia (NYT, 1995), one of the first examples of a systematic, imagery-based project to document and publicize human rights violations over a long period of time in a large region was conducted by the U.S. Department of State's Office of the Geographer and Global Issues' Humanitarian Information Unit (HIU). The HIU compiled information based on hundreds of VHR satellite images and published a map which showed the widespread destruction of villages in Darfur, Sudan (HIU, 2004). This information was passed to the U.N. and NGOs to assist in their efforts to monitor and document human rights violations in Darfur. By 2011 one especially well-funded human rights monitoring project, the Satellite Sentinel Project, had demonstrated the ability to purchase imagery from a constellation of VHR sensors and publicize the imagery from a location with a reported human rights violation in as little as 24 h (SatSentinel, 2011). Many other groups concerned with the human rights violations adopted similar analyst-intensive approaches to mostly visual interpretation of VHR imagery to monitor the conflict in Darfur and many other regions of the world (AAAS, 2013).

* Corresponding author. Tel.: +1 202 550 4080.
E-mail address: marxaj@umd.edu (A.J. Marx).
[1] Author is a foreign affairs analyst at the U.S. Department of State. He wrote this in his capacity as a graduate student at the University of Maryland. Any views expressed herein are solely his and do not necessarily represent those of the U.S. Department of State or the U.S. government.

0034-4257/$ – see front matter. Published by Elsevier Inc.
http://dx.doi.org/10.1016/j.rse.2013.05.006

Although the goals, production timeline, and publically released products of these human rights monitoring campaigns have been refined over the years, there are only a few examples of their methods evolving (Sulik & Edwards, 2010; Wolfinbarger & Drake, 2012) limiting the growth of remote sensing in the human rights community. Relying on manual analysis of VHR imagery over large areas and over long periods of time, these campaigns are cost prohibitive to all but the most well-funded monitoring efforts (Pisano, 2011). In the past, this work has been limited that it requires eyewitness reports, either from victims or international observers, before an organization can order satellite images to gather evidence of suspected violations. In the future social media, through mobile devices and internet penetration in many regions, promises to reduce the time gap between a reported human rights violation and an organization ordering imagery of that location.

Satellite and data-based early warning systems have been used since the 1970s for crop forecasts, severe storm prediction, and land use planning (Estes et al., 1980), but the development of early warning systems based on remotely sensed data to automatically alert users of a condition is relatively recent. One early warning system is the Drought Monitor, which uses data from the Advanced Very High Resolution Radiometer (AVHRR), in addition to other inputs, to provide weekly maps identifying where the emerging, persisting, and subsiding conditions of drought are located (Wilhite & Svoboda, 2000). The United States Agency for International Development (USAID) uses the Famine Early Warning System Network (FEWS NET) and takes this system one step further, incorporating AVHRR NDVI and meteorological satellites' rainfall data with other field-collected data to identify problems in the food supply system that could lead to famine or other food-insecure conditions (www.fews.net). FEWS NET products are available on a 10-day time period. In addition to these systems, the Webfire Mapper is part of the U.N.'s Foreign Agricultural Organization's Global Fire Information Management System (GFIMS). The Webfire Mapper was developed by the University of Maryland and supported by NASA, and it provides near real-time information on active fires worldwide, detected by the Moderate Resolution Imaging Spectroradiometer (MODIS) (Davies et al., 2009).

Because existing early warning systems rely on daily image acquisition, their value is limited to applications developed from coarse resolution (greater than 100 meter pixel size) imagery. The large pixel size of coarse resolution imagery makes definitive identification of most phenomena associated with human rights violations in this dryland ecosystem extremely challenging. Villages in arid environments can be relatively small (100 meter in diameter) and are constructed largely from local material, such as mud brick and roofs made from dry plant material, and show little contrast with the natural vegetation background in coarse resolution imagery. These differences have however been detected when the near infrared (NIR) band in VHR is utilized (Sulik & Edwards, 2010).

Research into applications from moderate resolution imagery (10–100 meter) has provided promising results, though no fully operational methods to monitor areas at risk of human rights violations have yet been developed. Prins (2008) demonstrated that Landsat Enhanced Thematic Mapper Plus (ETM+) could detect the destruction of villages in Darfur on an annual basis based on a visual analysis in the drop of albedo and Bromley (2010) links the Moderate Resolution Imaging Spectroradiometer (MODIS) sensor, which detects fire, with eyewitness reports of violence in Darfur. Landsat, Indian Remote-Sensing Satellite (IRS) and Système Pour l'Observation de la Terre (SPOT) imagery was used in 1999 to identify war-induced agricultural abandonment in Kosovo over a two-year period (Terres et al., 1999). Other studies have followed, demonstrating the ability of Landsat Thematic Mapper (TM) to detect agricultural abandonment in Bosnia in response to armed conflict (Witmer, 2008). Schimmer (2008) used coarse resolution MODIS and moderate resolution SPOT imagery to track an increase in vegetation cover and vigor in Darfur, which he linked to the displacement of people and their livestock. He noted that the spatial and temporal tracking of population displacement could provide important evidence to the scale and systematic nature of the violence—essential evidence in genocide trials.

Although previous studies have shown promising results, these methods are more suitable to scientific research than operational monitoring due to the considerable lag in time between the impact of the armed conflict on population and its identification in satellite imagery. In *Preventing Genocide: A Blueprint for U.S. Policymakers*, former U.S. Secretary of State Madeleine Albright writes that "at its most basic level, early warning means getting critical information to policymakers in time for them to take effective preventive action" (2008).

The strategic data acquisition plan for Landsat missions provides a suitable data source to serve as a prototype for development of such a warning system (Goward et al., 2006). The 16-day repeat cycle from Landsat 7 allowed us to collect an archive of images over Darfur between 1999 and 2011. While a combination of two Landsat satellites would have provided a better return frequency of 8 days, and thus greater opportunities for monitoring, this was not possible over Darfur region, as Landsat 5 is functioning in a very limited capacity and does not cover Darfur region at present and Landsat 7 has a scan line corrector (SLC) malfunction since mid-2003 leaving only 75% of each scene usable (http://landsat.gsfc.nasa.gov/about/landsat7.html). Subsequently, this project uses ETM+ as a prototype to develop such a warning system and to test its abilities. It may then be operationally deployable now that Landsat Data Continuity Mission (LDCM) is online as of February 2013.

Methods applied within an early warning system require an economically viable combination of frequent observations of the affected area, as well as an appropriate spatial resolution and spectral range for detecting the footprint of the phenomena associated with human rights violations. Currently, none of the available satellite systems meet these requirements, although, when functioning, the combination of Landsat 5 and 7 did provide free weekly observations of the area with data collected across visible, NIR, and short-wave infrared (SWIR) spectrum of electromagnetic radiation with limited resolving power of individual objects on the ground. In contrast, the price of individual VHR images, which frequently have limitations in spectral range of observations, makes many operational monitoring applications economically unfeasible. However, only VHR imagery allows for definitive identification of individual households and their condition in the Darfur region. Therefore, an early warning system for monitoring impacts of an armed conflict on population in Darfur requires a coordinated effort of moderate resolution imagery for early-stage possible identification and VHR imagery for verification.

In this paper we introduce a methodology for an early warning system using ETM+ that is designed to provide automated detection of the destruction of villages in arid environments. This remote sensing algorithm capitalizes on Landsat program's historical archive, radiometric stability, consistent calibration, and systematic observations by constructing a historic spectral baseline for each village in the study area (Markham et al., 2004). The application of the algorithm to the archived or operationally acquired Landsat and Landsat-like imagery identifies areas of high likelihood for village destruction in space-time and provides specifications for VHR image acquisition and analysis to verify impact and quantify the extent of damage at the individual household level.

2. Study area

In the late 1980s and 1990s, the Sudanese state of Darfur experienced clashes from both inter-tribal conflicts and armed insurrection by rebel groups. Beginning in 2003, the violence significantly escalated as government-supported militia groups, and later Sudanese military forces, attacked and destroyed thousands of villages. By September 2005 over 2 million people had fled the rural areas of Darfur to

camps and the larger towns, and another 200,000 had sought refuge in neighboring Chad (Petersen & Tullin, 2006). Refugees reported a similar pattern of attack: 1) their village was bombed, 2) soldiers and militia surrounded and entered the village, and 3) villages were looted and burned (U.S. Department of State, 2004).

In this approach we aim to link the visual descriptions of the environment obtained from satellite image analyses to causal human context following the framework proposed by Turner (2003). The proposed algorithm detects a remotely sensed phenomenon associated with a human rights violation. Specifically it detects a dramatic change in surface reflectance, indicating the burning of a village as it transitions from pre-burn materials (soil, deadwood, dead twigs and dead litter) to post-burn materials (soil, charwood, charred soil and ash). This approach provides a high degree of accuracy because, at the time in Darfur, such destruction was almost always due to an armed group violently removing a population and preventing their return by burning the village.

The study area consists of Landsat ETM+ path/row 179/51 in western Darfur, Sudan (Fig. 1). The land cover consists primarily of sparse vegetation (<15%) in the north, increasing to herbaceous vegetation grassland/savanna in the south (Defourny et al., 2006). It experiences heavy rain from the beginning of July to the end of October, with little rainfall in other months (Huffman et al., 2009). Cloud-cover corresponds to the wet months, with very few clouds in other months. While the widespread conflict in Darfur was distributed across 8 Landsat path/rows, this location was chosen because it contains the greatest concentration of destroyed villages in a one-year period (HIU, 2010).

3. Methodology

The input data for the algorithm includes Landsat surface reflectance data and the Humanitarian Information Unit's database of villages in Darfur (HIU, 2010). The methodology is presented in 3 parts: 1) image processing and village delineation, 2) algorithm flow, and 3) evaluation of 16 bands/indices derived from ETM+.

3.1. Image processing

The analysis of the change in surface reflectance caused by village destruction was performed using Landsat ETM+ images. Images were collected from four baseline years, ranging from 15 October 2000 to 27 December 2003 and the entire test year in 2004. There was a total of 21 SLC-on and 3 SLC-off images available for the baseline period, and 25 SLC-off for 2004 (http://earthexplorer.usgs.org). Of these, 17 images were not in the wet season or significantly affected by clouds and were used for the baseline, and eleven images in 2004 were used to test the algorithm (Table 1). The SLC corrector

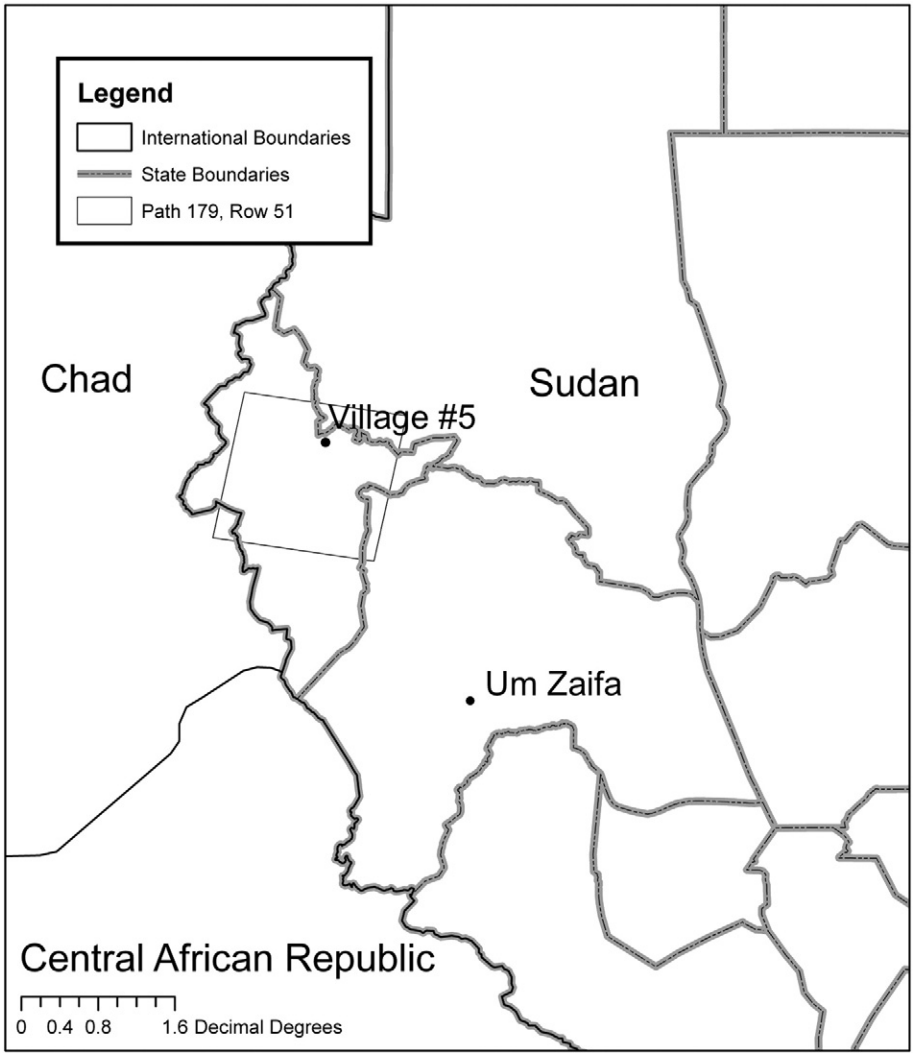

Fig. 1. The study area covers portions of West, North and South Darfur in western Sudan. Village #5 (Fig. 3) and Um Zaifa (Fig. 4) are indicated.

Table 1
Of the 39 images available for this path/row for the study period, 28 were used as they were not during the wet season or cloud covered.

Image number	USGS ID	Date	Used in study?	SLC
1	LE71790512000289EDC00	10/15/00	Yes	On
2	LE71790512000353SGS00	12/18/00	Yes	On
3	LE71790512001035SGS00	2/4/01	Yes	On
4	LE71790512001099EDC00	4/8/01	Yes	On
5	LE71790512001131SGS00	5/10/01	Yes	On
6	LE71790512001179EDC00	6/27/01	Yes	On
	LE71790512001243EDC00	8/31/01	No: wet season	On
	LE71790512001259SGS00	9/16/01	No: wet season	On
7	LE71790512001291SGS00	10/17/01	Yes	On
8	LE71790512001355SGS00	12/20/01	Yes	On
9	LE71790512002070EDC00	3/10/02	Yes	On
	LE71790512002118SGS00	4/28/02	No: clouds	On
	LE71790512002166SGS00	6/15/02	No: wet season	On
	LE71790512002230EDC00	8/18/02	No: wet season	On
	LE71790512002262EDC00	9/19/02	No: wet season	On
10	LE71790512002294SGS00	10/20/02	Yes	On
11	LE71790512002310SGS00	11/5/02	Yes	On
12	LE71790512002342SGS00	12/7/02	Yes	On
13	LE71790512003009SGS00	1/9/03	Yes	On
14	LE71790512003057SGS00	2/26/03	Yes	On
15	LE71790512003089EDC00	3/29/03	Yes	On
	LE71790512003265ASN01	9/22/03	No: wet season	Off
16	LE71790512003313ASN01	11/9/03	Yes	Off
17	LE71790512003361ASN01	12/27/03	Yes	Off
18	LE71790512004028ASN01	1/28/04	Yes	Off
19	LE71790512004044ASN01	2/13/04	Yes	Off
20	LE71790512004076ASN01	3/16/04	Yes	Off
21	LE71790512004092ASN01	4/1/04	Yes	Off
22	LE71790512004108ASN01	4/17/04	Yes	Off
23	LE71790512004124ASN01	5/3/04	Yes	Off
24	LE71790512004140ASN01	5/19/04	Yes	Off
25	LE71790512004156ASN01	6/4/04	Yes	Off
	LE71790512004236ASN01	8/23/04	No: wet season	Off
Images used in study				
	LE71790512004252ASN05	9/8/04	No: wet season	Off
	LE71790512004284ASN02	10/10/04	No: wet season	Off
	LE71790512004300ASN00	10/26/04	No: wet season	Off
26	LE71790512004316ASN00	11/11/04	Yes	Off
27	LE71790512004332ASN00	11/27/04	Yes	Off
28	LE71790512004348ASN00	12/13/04	Yes	Off

issues of ETM + imagery that began in May 2003 affect 25% percent of the footprint (Fig. 2). Landsat TM imagery is unavailable for this location because of the 1987 failure of the Tracking and Data Relay Satellite System (TDRSS) transmitter and because this path/row is not within range of a downlink station (Goward et al., 2006).

All Landsat terrain corrected (L1T) imagery were converted to surface reflectance using the Landsat Ecosystem Disturbance Adaptive Processing System (LEDAPS) (Wolfe et al., 2004). LEDAPS includes the Automated Cloud Cover Assessment (ACCA) algorithm, which creates an automatic cloud and cloud shadow mask based on Landsat bands 2 through 6 (Irish et al., 2006); however, ACCA does not perform well on semi-transparent clouds or cloud edges. Two baseline images (4/28/02 and 6/15/02) were not used due to cirrus cloud contamination that was not successfully masked with the ACCA.

Villages used in the case study were selected from the HIU's database of villages in Darfur (HIU, 2010). This database provides a center point (latitude and longitude) of all villages in Darfur and, where possible, its status by year (damaged, destroyed, or no damage). The extent of each village's structures was delineated manually from VHR imagery available in Google Earth and villages that are in areas significantly affected by the SLC errors are omitted from the study. All villages in the study area that were listed as destroyed in 2004 and not significantly affected by SLC errors were selected to test the algorithm—a total of 92 villages. These villages ranged in size from 25 to 262 Landsat pixels, or 750 to 7860 m^2. Another 92 villages were randomly selected from the hundreds of villages that were not in SLC error areas and were never listed as damaged or destroyed (Fig. 2). Five of these villages were smaller than 20 Landsat pixels or 600 m^2 and were removed from the control dataset, bringing the number to 87 villages.

While control villages were selected randomly, they tended to be smaller on average (2659 m^2) than villages that were identified as destroyed (3634 m^2). This is likely due to the fact that large destroyed villages have more eyewitnesses reporting attacks and are easier to identify through imagery. Control villages also tended to contain more biomass in their baseline observations (NIR = 0.32) than destroyed villages (0.28), indicating a greater density of built structures.

3.2. Band/index selection

We evaluated 16 different bands/indices derived from ETM + in the proposed algorithm. The band/index must produce a stable signal for each village throughout the baseline years with little variation between all observations in order for the algorithm to be effective. This prevents the incorrect identification of a destroyed village during the test year (i.e. commission error). However, the signal must be sensitive enough to identify the destruction of even small villages with sparsely built structures during the test year. We focused our analyses on testing a combination of surface reflectance and derived indices on two major components: 1) signal stability and 2) signal sensitivity.

3.2.1. Signal stability

Seventeen ETM + images from 15 October 2000 to 27 December 2003 created a population of observations for 179 different villages to evaluate 16 different bands/indices in their ability to produce a stable population of observations throughout the baseline years. These bands/indices includes Landsat ETM + bands 1 through 8, the normalized burn ratio (NBR) (Key & Benson, 2002), NDVI (Tucker, 1979), ETM+ bands 1 + 2 + 3 + 4 + 5 + 7, ETM+ bands 1 + 2 + 3, ETM+ bands 4 + 5, ETM+ bands 4 + 5 + 7, Tasseled Cap (TC) Brightness, TC Greenness, and TC Wetness (Huang et al., 2002).

For use in the proposed algorithm, a signal must be stable in all baseline observations, and not exhibit a strong seasonal green-up. While seasonal green-up is an important dynamic on the landscape, since the village itself is constructed from dead plant material and contains very little live vegetation within the boundaries, the effect of seasonal green-up is diminished within the boundaries of the settlement proper. And only recording the village's lowest 20% of pixels helps minimize the inclusion of green vegetation in the observation (Fig. 6). Additionally images from the months of June, July, August and September were not used because they correspond to the region's wet season (Huffman et al., 2009). Although these measures were taken, there is some evidence of village's producing lower reflectance scores following the wet season in October (Fig. 3) indicating that a seasonal green-up is minimized, but not fully negated.

A one-way ANOVA F-test statistic evaluated the relative stability of each band/index (Table 2) by measuring the between-group variability over within-group variability (Weisstein, 2003). In this algorithm, the variability between the 179 villages is divided by the variability within a single village (over up to 17 dates) so the larger the F-statistic, the more stable the signal is in comparison to observations across all villages.

The combination of NIR and SWIR1 (Landsat band 5 ~ 1.5 μm) produced the least amount of variability within a village compared to between villages. SWIR1 was the most stable single band followed by NIR. SWIR1, and to a lesser degree Wetness, produced high F-statistics because they are sensitive to moisture content of soil and vegetation. Because all observations were taken in the dry season, there was little change in moisture content within a village over time resulting in a stable signal (Fig. 3). NIR, which is sensitive to changes in biomass, also produced a stable population of observations because

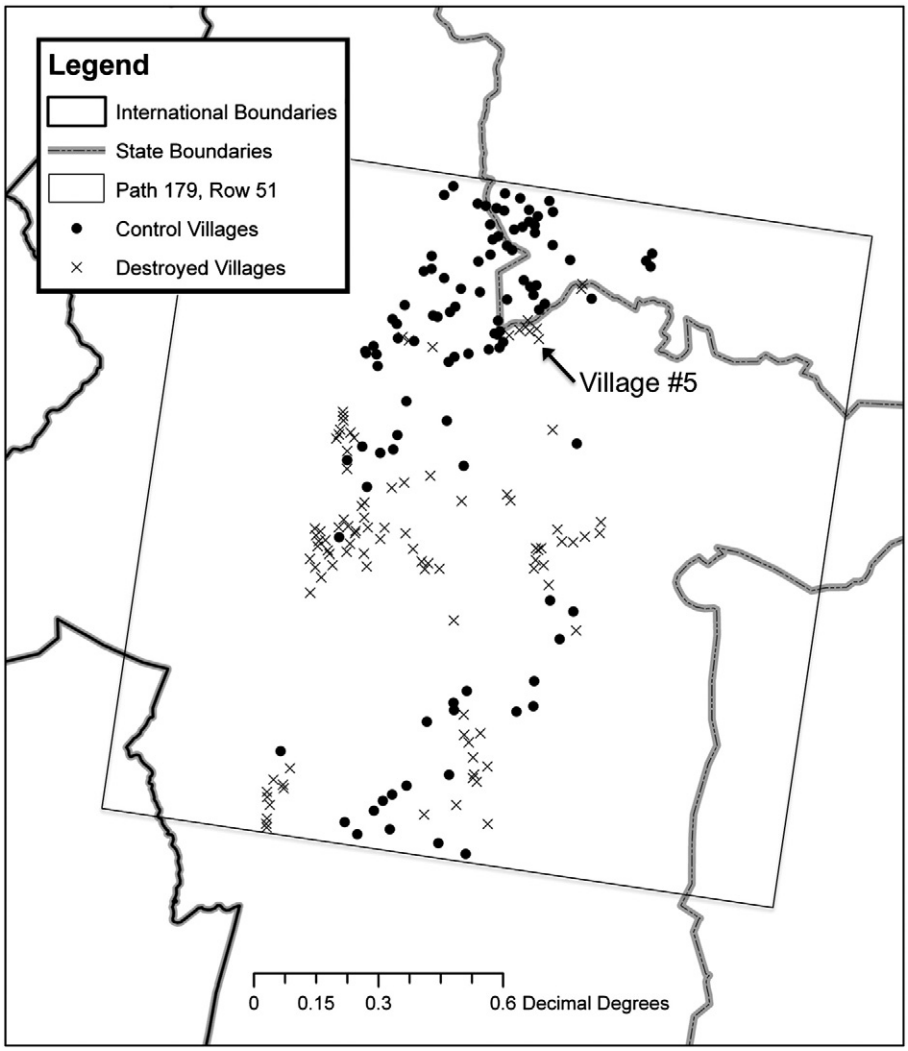

Fig. 2. Study area showing the study area in path/row 179/51, destroyed villages X, and control villages O. Villages in the study were chosen from the middle of the Landsat scene to minimize a lack of coverage due to scan lines. Village #5 is also indicated.

these arid villages are composed of dry plant material and bare, unvegetated ground that does not experience a strong seasonal green-up (Steidle, 2004) (Fig. 4). Visible bands, and indices that use visible bands, had low F-statistics, because they are more susceptible to atmospheric scattering in arid regions due to aerosols. While NBR is based on bands that were stable in this evaluation (NIR and SWIR1), NBR produced a very low F-statistics because it is a ratio designed to amplify differences in the signals.

3.2.2. Sensitivity

We then evaluated the 16 different metrics derived from ETM+ in their ability to detect the destruction of a village during the test year. For the 92 villages listed as destroyed for the test year of 2004 (HIU, 2010), each metric should produce at least one observation that is separated from the body of baseline observations, which is estimated as the detection of the village now destroyed (Fig. 5). Additionally for the 87 villages confirmed as not destroyed for 2004, there should be no observations that separate from the body of baseline observations.

The test year consisted of 11 ETM+ images in 2004 for the 179 villages. A one-tailed, student's t-test was used to determine if a village's observation during the test year was significantly lower than all observations during the baseline years (Weisstein, 2002). If the p value was less than a significance value of 0.0001, the village was considered destroyed (Table 3). There was assumed to be no variability in any single test observation, permitting a very low significance value of 0.0001.

ETM+'s visible bands and indices that use a combination of these bands, such as 1 + 2 + 3 + 4 + 5 + 7 and Red + Green + Blue, performed poorly with very high omission rates and very low commission rates. These metrics were not able to detect the signal for a village's destruction from the signal's noise, primarily because these metrics were not stable during the baseline years. SWIR2 (Landsat band 7 ~ 2.1 μm), Brightness, and Wetness performed better than the visible bands, but were also unable to separate the signal indicating a village's destruction from the metric's noise. By contrast, NBR, NDVI, and Greenness all produced very strong signals representing the destruction of a village, but because of the high variability of these indices (as indicated in their low F-statistics), they have very large commission error rates on control villages.

While SWIR1 and NIR + SWIR1 produced very stable populations of baseline observations, the signals produced for destroyed villages were insufficient for detection of destroyed villages as seen in their high omission rates.

ETM+ band 4 or NIR was the most effective metric tested for the algorithm. NIR produced a stable population of observations in the baseline years, as evidenced in a high F-statistic. This stability is also seen in the low commission rate for control villages in the test year. Additionally, the signal correctly representing the detection of a

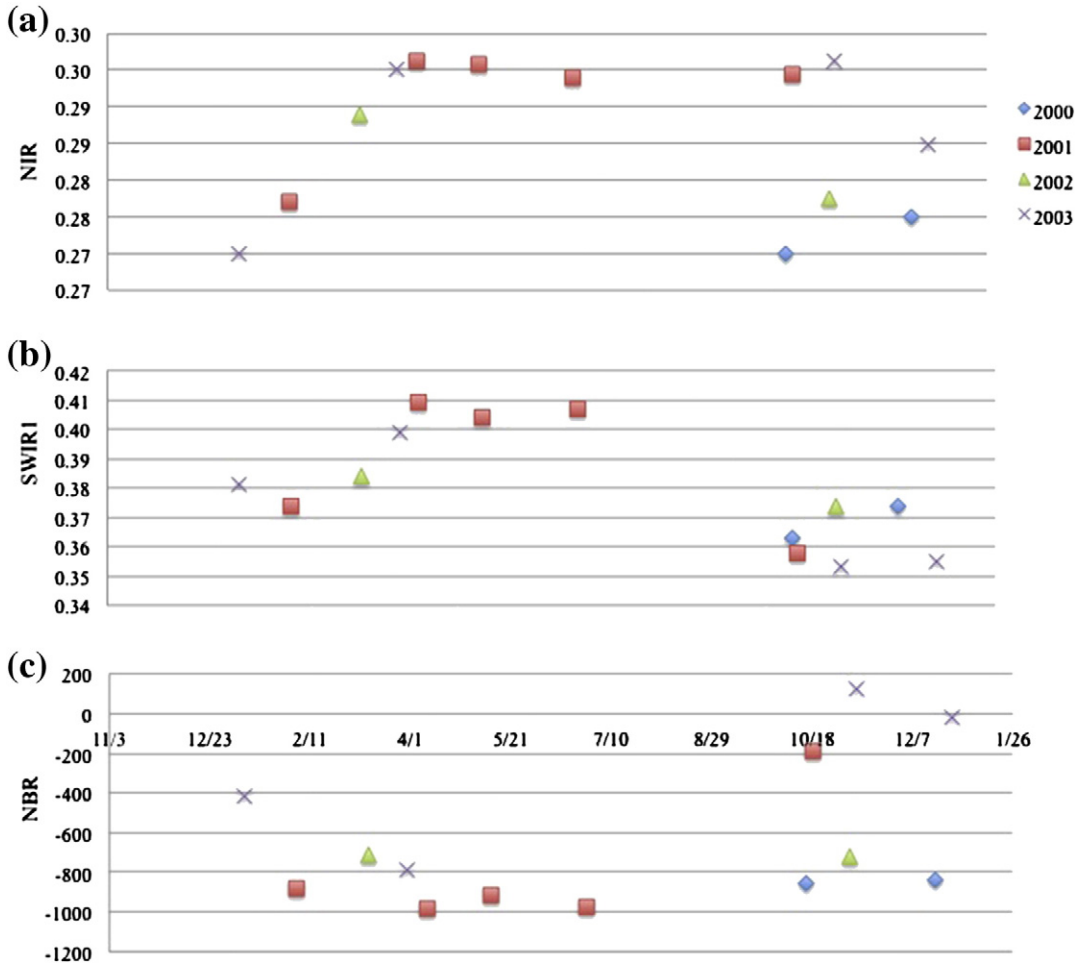

Fig. 3. Baseline observations in the algorithm for NIR (a), SWIR1 (b), and NBR (c) for test village #5 (lat: 13.453, lon: 23.254). SWIR1 and NIR provided the most stable population of observations in baseline years as measured by their F-statistic (Table 1). Observations were not available between July and October due to cloud cover.

destroyed village was strong enough for detection from the signal's noise, as evidenced by the low omission error rate (Table 2).

NIR likely performs well because villages in the study area are primarily constructed with deadwood and straw (Steidle, 2004) (Fig. 3).

Table 2
The stability of Landsat-based metrics in the algorithm was tested through an F-test statistic over baseline years. The variability between the 179 villages was divided by the variability within a single village so the larger the F-statistic the more stable the signal is in comparison to observations across all villages. ETM+ bands 4 and 5, and their sum, produced the most stable observations in the algorithm.

	F-statistic
Band 1	5.32
Band 2	11.91
Band 3	16.73
Band 4	34.62
Band 5	36.15
Band 6	0.29
Band 7	21.44
NBR	7.64
NDVI	4.32
1 + 2 + 3 + 4 + 5 + 7	23.68
1 + 2 + 3	12.26
4 + 5	37.19
4 + 5 + 7	32.60
TC brightness	23.91
TC greenness	6.66
TC wetness	28.35

When a village is destroyed there is a significant and persistent drop in dry plant material that is detectable in Landsat's NIR band. The NIR range is sensitive to internal plant structures, specifically the intercellular network of cellulose and the air trapped in-between those cells (Ustin et al., 2009). The change in NIR reflectance represents the transition in the village's structures from dead plant material to char and ash (U.S. Geological Survey, 2011). In grasslands or shrub areas,

Fig. 4. Um Zaifa, South Darfur, Sudan, burned on 10 December 2004. This village is not in the extent of the study area (lat: 11.083, lon: 24.676) (Petersen & Tullin, 2006). Photo: Brian Steidle © Courtesy of United States Holocaust Memorial Museum.

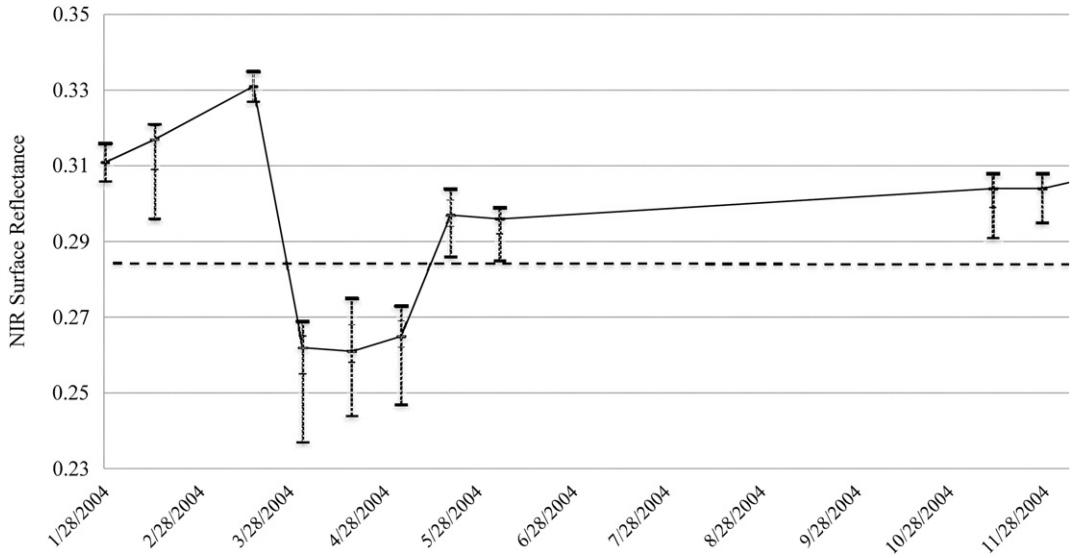

Fig. 5. Observations from 2004 for test village #5 (lat: 13.453, lon: 23.354) (HIU, 2010) show the sensitivity of NIR in the algorithm to detect a possible destruction; between the third and fourth observations in this case. The village's average for baseline observations is shown as a dashed line.

which closely mimic the land cover in these villages, studies have produced similar results showing NIR isolines significantly separating in prefire and postfire situations (Roy et al., 2006).

3.3. Algorithm flow

Two satellite images from two dates, spaced one year apart (or an annual multiples thereof), are most often used in change detection because they minimize discrepancies in reflectance caused by seasonal vegetation fluxes and sun angle differences (Coppin et al., 2004). This has been shown to be very effective in detecting forest disturbance using Landsat TM and ETM+ (Kennedy et al., 2007). Temporal trajectory analysis is less accurate, attempting to identify changes within a calendar year by building seasonal development curves or profiles of the study area. Changes are detected when the study area departs from the baseline curve (Kasischke & French, 1995).

This algorithm proposes new methodology by detecting if a village's observation at each new pass of the sensor during the test year is significantly lower than the body of observations from baseline years (Fig. 6). Observations are calculated averaging the lowest 20% of the village's pixels. During the test year, a one-tailed, student's t-test ($p = 0.0001$) is used to determine if village's observation is significantly lower than the historical body of its observations (Weisstein, 2002). If so, it alerts as possibly destroyed.

This methodology is possible in part because LEDAPS is effective at image-to-image normalization and geo-registration, reducing noise in the 8-bit sensor (Markham et al., 2004). This allows for precise pixel alignment of all of images used in the algorithm and reduces differences in the images caused by atmospheric affects. The method of comparing a village's observation to a stack of its previous observations increases the sensitivity of the algorithm by eliminating differences between villages such as local land cover and the density of build structures. This is similar to Loboda et al. (2007), increasing the sensitivity of fire detection methods by modifying the algorithm based on the local environment.

Table 3
Landsat-based metrics were tested in the algorithm against the reference database. A one-tailed, student's t-test was used to determine if any single, test year observation was lower than that village's baseline observations. There was assumed to be no variability in the single test observation, permitting an α of 0.0001.

	Omission error	Commission error	Accuracy
Band 1	88.0%	16.1%	46.9%
Band 2	90.2%	3.4%	52.0%
Band 3	92.4%	5.7%	49.7%
Band 4	17.4%	13.8%	84.4%
Band 5	65.2%	14.9%	59.2%
Band 6	57.6%	77.0%	33.0%
Band 7	82.6%	4.6%	55.3%
NBR	16.3%	47.1%	68.7%
NDVI	17.4%	72.4%	55.9%
1 + 2 + 3 + 4 + 5 + 7	84.8%	10.3%	51.4%
1 + 2 + 3	89.1%	9.2%	49.7%
4 + 5	42.4%	12.6%	72.1%
4 + 5 + 7	73.9%	10.3%	57.0%
TC brightness	79.3%	9.2%	54.7%
TC greenness	19.6%	77.0%	52.5%
TC wetness	72.8%	26.4%	49.7%

4. Validation dataset and methodology

The validation reference base used to test the algorithm's performance on these 197 villages is the U.S. Department of State's Office of the Geographer and Global Issues' HIU database (HIU, 2010). This database is a compilation of information based on hundreds of VHR satellite images that lists the location of villages in Darfur, Sudan and their annual status as either damaged, destroyed, or no damage. A destroyed village is defined as confirmed evidence of complete destruction of the village. Villages where the date of damage could not be determined (those listed in the database as "damaged at any time") were not included in this study. We computed the confusion matrix and calculated commission and omission errors and the overall accuracy (Table 2).

5. Results

The use of ETM+ band 4 in the algorithm correctly detected 84% of the villages identified as destroyed by the HIU database in 2004. The algorithm incorrectly detected 14% of the control villages as being destroyed. Increasing the significance level to 0.0005 reduces the omission rate, but it also significantly increases the number of villages incorrectly detected as destroyed. While there is limited VHR imagery of this area in 2004 and subsequent years, a survey of available VHR imagery from 2005 to 2007 confirmed that at least

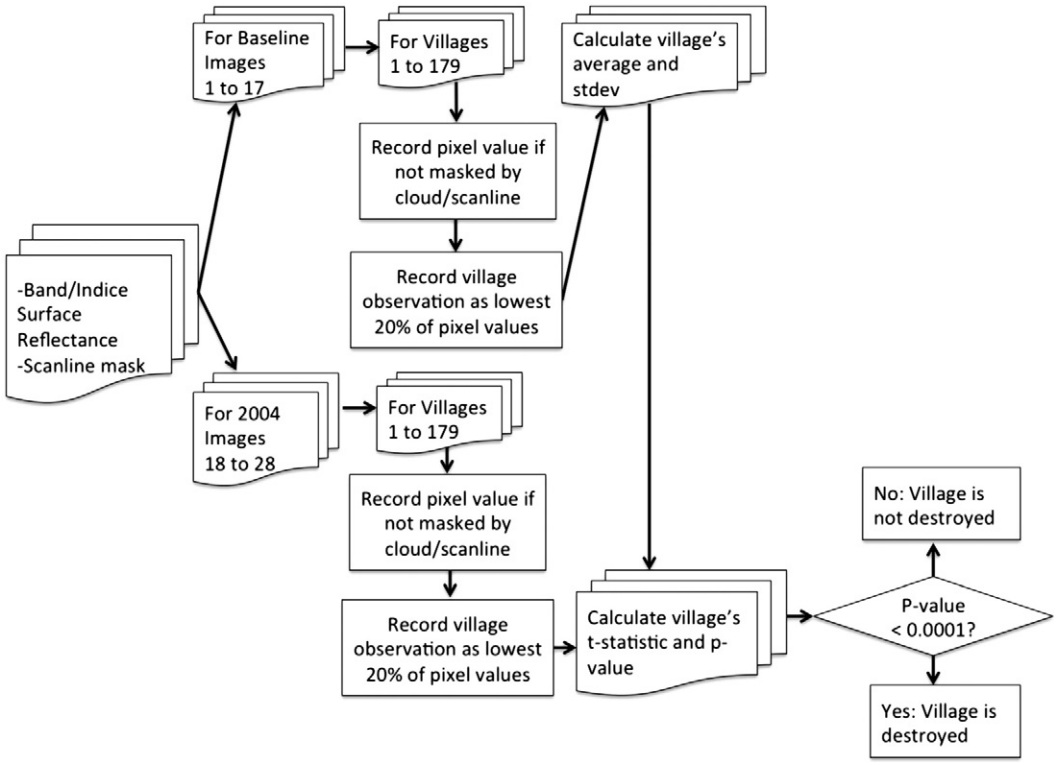

Fig. 6. Landsat ETM + destroyed village detection algorithm process stages. All images are converted to surface reflectance and scan line and cloud masks are created. The first seventeen images are used to create a baseline average and standard deviation for each of the 179 villages. A village's observation for an image is calculated as the average of the village's lowest 20% pixel values. A village's observation for images 18 to 28 are tested against its baseline images through a t-test. If the p-value is less than 0.0001 the village is detected as possibly destroyed.

six of the eight control villages identified as destroyed in 2004 were never destroyed.

There is not a single identified factor for why twelve of the 87 control villages had an observation in the test year that was significantly lower than its body of baseline observations. These villages had a slightly higher baseline average and standard deviation (0.34 and 0.024, respectively) than all control villages (0.32 and 0.022, respectively). While small control villages (less than 50 pixels) were more likely to have commission errors, large control villages (greater than 180 pixels) had few commission errors (Table 4). These large villages tend to have lower NIR averages and less NIR variability throughout the year, likely because they are more densely built and reflect seasonal green-ups less than small villages. There was no temporal correlation, such as the first image after the wet season, for when a control village registered a commission error. It is most likely that these few control villages which were detected by the algorithm as being possibly destroyed in the test year was because of anthropological reasons such as the burning of agricultural plots very close or within the village's border, or because fences or other structures were destroyed on a limited basis in the village.

16 of 92 villages listed as destroyed in 2004 (HIU, 2010) were not detected as destroyed using our approach. Similar to the villages that had commission errors, villages with omission errors had higher baseline reflectances and standard deviations (0.28 and 0.016, respectively) than those where a burn was detected (0.29 and 0.017, respectively), indicating villages with more seasonal plant growth. A survey of available VHR imagery confirmed that 13 of these 16 villages were destroyed sometime before 2007. One of the villages was identified as intact in the VHR imagery, indicating shortcomings in the reference database. Further visual inspection of Landsat ETM + imagery indicates that three of these villages were destroyed in the end of 2003, effectively reduced omission error to 12 of 88, or 14%.

During the wet season, there is a five-month gap in satellite coverage from 4 June to 11 November 2004 due to cloud cover. While village destruction declines during this time due to impassable roads (Petersen & Tullin, 2006), other omission errors may be because villages were destroyed during this time period. While the HIU database was used because it contained the largest collection of villages identified as destroyed, the few errors in the database reveal that a study of its accuracy using smaller databases compiled from eyewitness reporting (Petersen & Tullin, 2006; Raleigh et al., 2010) would be valuable for future studies that cover the entire Darfur conflict.

Table 4
Omission and commission errors by village size. The control village data set had a larger number of smaller villages and a higher percentage of commission errors. Large villages (over 179 pixels) had few errors. While control villages were selected randomly, they tended to be smaller on average than destroyed villages that have more eyewitnesses reporting attacks and are easier to identify through imagery.

Destroyed villages			Not destroyed villages	
Pixels	Total	Omission error	Total	Commission error
20–49	9	1	26	7
50–99	28	6	33	4
100–179	41	8	22	0
180–285	14	1	6	1

6. Conclusion

Currently few organizations are able to conduct human rights monitoring campaigns because existing methods are prohibitively costly and labor-intensive. The presented algorithm provides an approach that reduces the cost of human rights monitoring campaigns in arid regions by focusing the purchase of VHR imagery and analysis to areas

that have been alerted by moderate resolution imagery sensors. This does not eliminate the costs however. While the moderate resolution imagery and imagery pre-processing software (LEDAPS) used to run the algorithm is available online at no cost to users, VHR imagery purchases to confirm village destruction, and trained analysts to interpret the results still make this a costly monitoring program to implement.

Our results show that the approach provides a reliable detection of village destruction in 84% of the cases with very few false alarms. As a warning mechanism, the demonstrated approach provides a worst-case lag of 16 days (assuming no cloud cover), the revisit rate of ETM+. The Landsat Data Continuity Mission (LDCM), launched in 2013, in combination with ETM+, would reduce the warning lag by up to eight days. Additionally, other moderate resolution sensors, such as India's ResourceSat-1 Advanced Wide Field Sensor (AWiFS), have been shown to be interchangeable with Landsat in earth-observing applications (Goward et al., 2012). The inclusion of other moderate resolution sensors to this algorithm could also be used to improve accuracy by modifying the algorithm to detect when two sequential observations are significantly different from baseline observations.

The threshold, developed within this algorithm, is aimed at monitoring villages in Darfur, Sudan in 2004, and is specific to this region's building materials as well as the methods of the perpetrators (e.g. the burning of villages). While the proposed method is generalizable to broader geographic regions it relies on similar definition and nature of human rights violation that results in burning of residencies within the village. However, the strength of the proposed approach lies in limiting the threshold analysis to unique conditions within individual villages rather than selecting a single value across the region thus bypassing the overgeneralization bias common for remote sensing analyses (Turner, 2003). The expansion of this approach necessitates the identification of an observable signal in the region of interest that indicates a possible international humanitarian law violation. We plan to expand the algorithm to other regions following the overall framework presented in this paper. In the future, data from a constellation of moderate resolution sensors could provide a low-cost and continual monitoring of regions at-risk of international humanitarian law violations.

References

AAAS (2013). *AAAS scientific responsibility, human rights and law program: Geospatial technologies and human rights.* : AAAS Science and Policy Program (http://shr.aaas.org/geotech/cases.shtml#AAAS_cases, last accessed 04/01/2013).

Bromley, L. (2010). Relating violence to MODIS fire detections in Darfur, Sudan. *International Journal of Remote Sensing*, *31*(9), 2277–2292.

Coppin, P., Jonckheere, I., Nackaerts, K., Muys, B., & Lambin, E. (2004). Review ArticleDigital change detection methods in ecosystem monitoring: A review. *International Journal of Remote Sensing*, *25*, 1565–1596.

Davies, D. K., Ilavajhala, S., Wong, M. M., & Justice, C. O. (2009). Fire information for resource management system: Archiving and distributing MODIS active fire data. *IEEE Transactions on Geoscience and Remote Sensing*, *47*, 72–79.

Defourny, P., Vancutsem, C., Bicheron, P., Brockmann, C., Nino, F., Schouten, L., et al. (2006). GLOBCPVER: A 300m global land cover product for 2005 using ENVISAT MERIS Time Series. *Proceedings of ISPRS Commission VII Mid-Term Symposium: Remote Sensing: from Pixels to Processes* (pp. 59–62) Enschede (NL) (8–11 May, 2006).

Estes, J. E., Jensen, J. R., & Simonett, D. S. (1980). Impacts of remote sensing on US geography. *Remote Sensing of Environment*, *10*, 43–80.

Goward, S., Arvidson, T., Williams, D., Faundeen, J., Irons, J., & Franks, S. (2006). Historical record of Landsat global coverage: Mission operations, NSLRSDA, and international cooperator stations. *Photogrammetric Engineering and Remote Sensing*, *72*, 1155.

Goward, S., Chander, G., Pagnutti, M., Marx, A., Ryan, R., Thomas, N., & Tetrault, R. (2012). Complementarity of resourcesat-1 AWiFS and Landsat TM/ETM+ sensors. *Remote Sensing of Environment*, *123*, 41–56.

HIU (2004). *Sudan (Darfur)–Chad border region confirmed damaged and destroyed villages.* Washington, D.C.: U.S. Department of State, Humanitarian Information Unit (https://hiu.state.gov/Pages/Africa.aspx).

HIU (2010). *Darfur, Sudan: Confirmed damaged and destroyed villages, February 2003–December 2009.* Washington, D.C.: U.S. Department of State (https://hiu.state.gov/Pages/Africa.aspx).

Huang, C., Wylie, B., Yang, L., Homer, C., & Zylstra, G. (2002). Derivation of a tasselled cap transformation based on Landsat 7 at-satellite reflectance. *International Journal of Remote Sensing*, *23*, 1741–1748.

Huffman, G. J., Adler, R. F., Bolvin, D. T., & Gu, G. (2009). Improving the global precipitation record: GPCP version 2.1. *Geophysical Research Letters*, *36*, L17808.

Irish, R. R., Barker, J. L., Goward, S. N., & Arvidson, T. (2006). Characterization of the Landsat-7 ETM automated cloud-cover assessment (ACCA) algorithm. *Photogrammetric Engineering and Remote Sensing*, *72*, 1179–1188.

Kasischke, E. S., & French, N. H. F. (1995). Locating and estimating the areal extent of wildfires in Alaskan boreal forests using multiple-season AVHRR NDVI composite data. *Remote Sensing of Environment*, *51*, 263–275.

Kennedy, R. E., Cohen, W. B., & Schroeder, T. A. (2007). Trajectory-based change detection for automated characterization of forest disturbance dynamics. *Remote Sensing of Environment*, *110*, 370–386.

Key, C., & Benson, N. (2002). Measuring and remote sensing of burn severity. In K. C. R. L. F. Neuenschwander, & G. E. Goldberg (Eds.), *Proceedings of the Joint Fire Science Conference (pp. 02-11). Boise, Idaho 15–17 June, 1999. University of Idaho and the International Association of Wildland Fire*, *Vol. II.* (pp. 284).

Loboda, T., O'Neal, K., & Csiszar, I. (2007). Regionally adaptable dNBR-based algorithm for burned area mapping from MODIS data. *Remote Sensing of Environment*, *109*, 429–442.

Markham, B. L., Thome, K. J., Barsi, J. A., Kaita, E., Helder, D. L., Barker, J. L., & Scaramuzza, P. L. (2004). Landsat-7 ETM+ on-orbit reflective-band radiometric stability and absolute calibration. *IEEE Transactions on Geoscience and Remote Sensing*, *42*, 2810–2820.

Marx, A., & Goward, S. (2013). Remote sensing in human rights and international humanitarian law monitoring: concepts and methods. *Geographical Review*, *103*, 100–111.

NYT [New York Times] (1995). *Massacre in Bosnia; Srebrenica: The Days of Slaughter*. New York Times, 29 October. (www.nytimes.com/1995/10/29/world/massacre-in-bosnia-srebrenica-the-days-of-slaughter.html).

OHCHR [Office of the High Commissioner for Human Rights] (2001). *Training manual on human rights monitoring.* New York: United Nations.

Petersen, A., & Tullin, L. (2006). *The scorched earth of Darfur: Patterns in death and destruction reported by the people of Darfur. January 2001–September 2005.* Copenhagen: Bloodhound.

Pisano, F. (2011). *Director, UNITAR'S operational satellite applications programme. Interview with the authors. Washington, DC.*

Prins, E. (2008). Use of low cost Landsat ETM+ to spot burnt villages in Darfur, Sudan. *International Journal of Remote Sensing*, *29*(4), 1207–1214.

Raleigh, C., Linke, A., Hegre, H., & Karlsen, J. (2010). Introducing ACLED: An armed conflict location and event dataset special data feature. *Journal of Peace Research*, *47*, 651–660.

Roy, D. P., Boschetti, L., & Trigg, S. N. (2006). Remote sensing of fire severity: Assessing the performance of the normalized burn ratio. *IEEE Geoscience and Remote Sensing Letters*, *3*, 112–116.

SatSentinel (2011). The world is watching because you are watching. (www.satsentinel.org).

Schimmer, R. (2008). Tracking the genocide in Darfur: Population displacement as recorded by remote sensing. *Working paper* (pp. 36). Yale Genocide Studies Program.

Steidle, B. (2004). *Um Zaifa, Darfur. 10 December 2004. Courtesy of United States Holocaust Memorial Museum.*

Sulik, J., & Edwards, S. (2010). Feature extraction for Darfur: Geospatial applications in the documentation of human rights abuses. *International Journal of Remote Sensing*, *31*(10), 2521–2533.

Terres, J., Biard, F., & Darras, G. (1999). *Kosovo: Assessment of changes of agricultural land use areas for the 1999 crop campaign using satellite data.* Ispra, Italy: Space Applications Institute Report, Joint Research Centre.

Tucker, C. J. (1979). Red and photographic infrared linear combinations for monitoring vegetation. *Remote Sensing of Environment*, *8*, 127–150.

Turner, M. D. (2003). Methodological reflections on the use of remote sensing and geographic information science in human ecological research. *Human Ecology*, *31*(2), 255–279.

U.S. Department of State (2004). *Documenting Atrocities in Darfur.* State Publication 11182 (http://2001-2009.state.gov/g/drl/rls/36028.htm, last accessed April, 15 2013).

U.S. Geological Society (2011). *Spectral library: Western Montana.* Joint Fire Science Program.

Ustin, S., Jacquemoud, S., Palacios-Orueta, A., Li, L., & Whiting, M. (2009). Remote sensing based assessment of biophysical indicators for land degradation and desertification. *Recent advances in remote sensing and geoinformation, processing for land degradation assessment* (pp. 15–44). London: ISPRS Series.

Weisstein, E. W. (2002). *CRC Concise Encyclopedia of Mathematics* (2nd ed.) Hoboken: CRC press. ISBN 1420035223.

Weisstein, E. W. (2003). *CRC concise encyclopedia of mathematics.* CRC press.

Wilhite, D. A., & Svoboda, M. D. (2000). Drought early warning systems in the context of drought preparedness and mitigation. *Early warning systems for drought preparedness and drought management* (pp. 1–16).

Witmer, F. D. W. (2008). Detecting war-induced abandoned agricultural land in northeast Bosnia using multispectral, multitemporal Landsat TM imagery. *International Journal of Remote Sensing*, *29*(10), 3805–3831.

Wolfe, R., Masek, J., Saleous, N., & Hall, F. (2004). LEDAPS: Mapping North American disturbance from the Landsat record. *Geoscience and remote sensing symposium, 2004. IGARSS '04. Proceedings. 2004 IEEE International.*

Wolfinbarger, S., & Drake, J. (2012). *Eyes on Nigeria: Technical report industrial gas flaring.* Washington, D.C.: American Association for the Advancement of Science, Scientific Responsibility, Human Rights and Law Program (shr.aaas.org/geotech/flaring.shtml).